Acta Oceanol. Sin., 2017, Vol. 36, No. 9, P. 108–113
DOI: 10.1007/s13131-017-1116-x
http://www.hyxb.org.cn
E-mail: hyxbe@263.net

Nonparametric estimations of the sea state bias for a radar altimeter

MIAO Hongli[1]*, JING Yujie[1], JIA Yongjun[2], LIN Mingsen[2], ZHANG Guoshou[1], WANG Guizhong[1]

[1] College of Information Science and Engineering, Ocean University of China, Qingdao 266100, China

[2] National Satellite Ocean Application Service, State Oceanic Administration, Beijing 100081, China

Received 23 May 2016; accepted 25 April 2017

Abstract

To estimate the sea state bias (SSB) for radar altimeter, two nonparametric models, including a Nadaraya-Watson (NW) kernel estimator and a local linear regression (LLR) estimator, are studied based on the Jason-2 altimeter data. Selecting from different combinations of the Gaussian kernel function, spherical Epanechnikov kernel function, a fixed bandwidth and a local adjustable bandwidth, it is observed that the LLR method with the spherical Epanechnikov kernel function and the local adjustable bandwidth is the optimal nonparametric model for the SSB estimation. The comparisons between the nonparametric and parametric models are conducted and the results show that the nonparametric model performs relatively better at high-latitudes of the Northern Hemisphere. This method has been applied to the HY-2A altimeter as well and the same conclusion can be obtained.

Key words: radar altimeter, sea state bias, significant wave height, wind speed, nonparametric model, parametric model

Citation: Miao Hongli, Jing Yujie, Jia Yongjun, Lin Mingsen, Zhang Guoshou, Wang Guizhong. 2017. Nonparametric estimations of the sea state bias for a radar altimeter. Acta Oceanologica Sinica, 36(9): 108–113, doi: 10.1007/s13131-017-1116-x

1 Introduction

The radar altimeter produces various errors during the height measurements. The sea state bias (SSB) is generally accounted for 1/3 of the total error in the Jason-1 altimeter, and has taken place of the orbital error as the largest error source due to the development of precise orbit determination technologies (Fu and Cazenave, 2001; Wang et al., 2014a, b). When the radar altimeter transmits pulses toward a nadir point, the curvature of wave crests is usually larger than that of wave troughs. The results in the backscattered power measured by the altimeter from the wave troughs are greater than that from the wave crests. The mean scattering surface biases toward the wave troughs from a mean sea level, so that the mean sea level measured by altimeters is lower than the real one. The difference between the measured and real mean sea surfaces is called the electromagnetic bias. In addition, there are a skewness bias, which is caused by mismatching between the mean scattering surface and the median scattering surface because specular scattering in sea level does not follow the Gaussian distribution, and a tracker bias in determination of the median height by tracker. These three errors are all known as the sea state bias. At present, the SSB estimation still relies on empirical methods, including both parametric models and nonparametric models (Li et al., 2013).

The parametric model for the SSB estimation based on the Taylor expansion of the significant wave height (SWH) and a wind speed is simple, intuitive, easy to use and its extensionality is good (Miao et al., 2015; Wang et al., 2014a, b). Due to the lack of true SSB values, the model coefficients are determined by the sea surface height (SSH) differences, the SWH differences and the wind speed differences at crossover points or along collinear tracks. However, when calculating the SSB, only the SWH and the wind speed can be used. Therefore, the parametric model is not based on a true least square method, which may cause an error in the model coefficients learning (Vandemark et al., 2002).

The nonparametric models based on the technology of kernel smoothing can avoid the problems existing in the parametric models. The nonparametric model characterized in the form of regression function has no constraints on the distribution of the estimated variables. Furthermore, the curve fitting using the nonparametric model meets the principle of least squares very well and can describe subtle changes between the variables. Therefore, the SSB estimation accuracy at the northern latitudes, where the sea state is complicated due to the influence of the land, is significantly improved over the parametric model (Gaspar et al., 2002; Labroue et al., 2004; Scharoo and Lillibridge, 2004; Ye et al., 2015).

The nonparametric estimations mainly include the Nadaraya-Watson kernel estimation (NW), a local linear regression estimation (LLR), a K-neighbor estimation, an orthogonal sequence estimation and a polynomial spline estimation, etc (Tran et al., 2010a, b ; Feng et al., 2010; Rami et al., 2011). In this paper, we focus on the first two methods, and the results are compared with the parametric models.

2 Modeling principle

An uncorrected sea surface height SSH′ (h') can be expressed as

$$h' = b + h_g + h_d + \varepsilon', \tag{1}$$

Foundation item: The National Key R&D Program of China under contract No. 2016YFC1401004; the National Natural Science Foundation of China under contract Nos 41406207, 41176157 and 41406197.
*Corresponding author, E-mail: oumhl@ouc.edu.cn

where b is the SSB, h_g is the geoid, h_d is the dynamic topography, and ε' is the sum of all height measurement errors except the SSB (Li et al., 2013).

The geoid is the largest signal with an order of meters to tens of meters. The geoid is a time-invariant signal which can be eliminated by carrying out the difference between measurements at crossover points. Adopting the discrepancy between individual measurements at different time, Eq. (1) can be expressed directly as

$$h_2' - h_1' = (b_2 - b_1) + \varepsilon, \tag{2}$$

where the subscripts 1 and 2 denote measurements at the crossover point when the altimeter ascending and descending, respectively. Parameter ε is the mean error (or residual) which includes the time-variation of the dynamic topography and other measurement errors except the SSB (Gasper et al., 1994).

The research shows that the SSB is closely related to the SWH and the wind speed. Hence, if x is a binary variable of the SWH and the wind speed (U), $x = (h_s, U)$, where h_s is the SWH, the SSB can be determined as

$$b = \varphi(x). \tag{3}$$

Setting $y = h_2' - h_1'$, Eq. (2) can be rewritten as

$$y = \varphi(x_2) - \varphi(x_1) + \varepsilon. \tag{4}$$

Because the mean error is a zero-mean noise, the conditional expectation of y is

$$E[y\,|x_2 = x] = \varphi(x) - E[\varphi(x_1)\,|x_2 = x]. \tag{5}$$

For kernel functions, the conditional expectation $E[\zeta_i\,|x]$ of the kernel estimator $\hat{r}(x)$ is a weighted mean of the measurements ζ_i, and the weight is a decreasing function of a distance between x and x_i (Gaspar and Florens, 1998),

$$\hat{r}(x) = \sum_{i=1}^{n} \zeta_i \alpha_n (x - x_i), \tag{6}$$

where α_n is a weighted function which is associated with n and satisfies the following condition:

$$\sum_{i=1}^{n} \alpha_n (x - x_i) = 1. \tag{7}$$

By using Eq. (6) and a set of n altimeter crossover measurements, Eq. (5) can be rewritten as

$$\varphi(x) = \sum_{i=1}^{n} y_i \alpha_n (x - x_{2i}) + \sum_{i=1}^{n} \varphi(x_{1i}) \alpha_n (x - x_{2i}). \tag{8}$$

Equation (8) provides a practical method to estimate $\varphi(x)$ for any vector $\vec{x}$, provided that the value of $\varphi(x_1)$ is known, where, $\varphi(x_1)$ is the estimated value of the SSB at the crossover point when the altimeter ascending.

The following two methods can be used to determine the weighted function α_n (Gaspar et al., 2002).

(1) the Nadaraya-Watson kernel estimation (NW)

$$\alpha_n (x - x_i) = \frac{K\left(\dfrac{x - x_i}{h_n}\right)}{\sum\limits_{i=1}^{n} K\left(\dfrac{x - x_i}{h_n}\right)}, \tag{9}$$

where $K(\cdot)$ is a kernel function; $\alpha_n(x - x_i)$ is the (1×n) weighted vector, n is the number of crossover points, and h_n is the bandwidth vector; and the index n indicates that the bandwidth depends on the number of measurements.

(2) The local linear regression estimation (LLR)

$$\alpha_n(\boldsymbol{x} - x_i) = e_1^{\mathrm{T}} (\boldsymbol{X}_{\mathrm{D}}^{\mathrm{T}} \boldsymbol{W} \boldsymbol{X}_{\mathrm{D}})^{-1} \boldsymbol{X}_{\mathrm{D}}^{\mathrm{T}} \boldsymbol{W}, \tag{10}$$

where $\boldsymbol{e}_1^{\mathrm{T}} = (1, 0, 0)$, is the (1×3) unit vector; $\boldsymbol{X}_{\mathrm{D}} = (1, \boldsymbol{x} - \boldsymbol{x}_i)$, is the ($n$×3) matrix; and $\boldsymbol{W} = M\left\{K\left(\dfrac{x - x_i}{h_n}\right)\right\}$, is the ($n$×$n$) diagonal matrix, M is diagonal matrix operator. Thus $\alpha_n(x - x_i)$ is the (1×n) weighted vector.

The above two methods both involve the problems how to select the kernel function $K(\cdot)$ and bandwidth h_n. The kernel function $K(\cdot)$ is a symmetric scalar function with $\int K(\boldsymbol{x})\mathrm{d}\boldsymbol{x} = 1$, which is usually selected as a probability density function.

In this paper, for $x = (U, h_s)$ in which h_s is the SWH, h_n= (h_U, h_{h_s}) is the bandwidth vector. Two forms of $K(\cdot)$ are selected:

(1) the Gaussian kernel function. In two-dimensional case, the function is

$$K\left(\frac{x - x_i}{h_n}\right) = \frac{1}{2\pi h_U h_{h_s}} \exp\left[\frac{-(U - U_i)^2}{2h_U^2}\right] \times \exp\left[\frac{-(h_s - h_{si})^2}{2h_{h_s}^2}\right]; \tag{11}$$

(2) the spherical Epanechnikov kernel function. In two-dimensional case, the function is

$$K\left(\frac{x - x_i}{h_n}\right) = \max\left\{0, \frac{2}{\pi h_U h_{h_s}} \times \left[1 - \left(\frac{U - U_i}{h_U}\right)^2 - \left(\frac{h_s - h_{si}}{h_{h_s}}\right)^2\right]\right\}. \tag{12}$$

There are two choices for the bandwidth h_n. One is the global bandwidth (h_Global):

$$h_n = C\sigma_x n^{-1/5}, \tag{13}$$

where σ_x is the standard deviation of the wind speed or SWH; and C is an empirical value of 1.06 (Gaspar and Florens, 1998). The other one is the locally variable bandwidth (h_Local),

$$h_n = h_{x0}[n(x)/\overline{n(x)}]^{-1/6}. \tag{14}$$

where h_{x0} is a reference bandwidth of the wind speed or SWH. All the wind speed and the SWH at the crossover points are divided

into groups according to a certain interval, $n(x)$ is the number of measurements in the group of x. $\overline{n(x)}$ is the mean value of $n(x)$ in each group. The group bandwidth is variable and negatively related to the number of measurements (Gaspar et al., 2002).

3 Model establishment

3.1 *Data set determination*

The nonparametric models have large computational costs because of complex matrix operations. So, proper modeling data volume cannot only ensure the accuracy but also improve the efficiency. The segmented fitting method of track was adopted to extract crossovers data from Cycles 207, 218, 225 and 234 of Jason-2. The nonparametric model with the NW estimation, the Gaussian kernel function and the global bandwidth was established and compared based on these data sets. The explained variance (D) changes little even the data set increasing to four cycles, as shown in Table 1. There is no significant improvement for the accuracy of the SSB estimation with increasing data volume. Therefore, only the Cycle 207 crossovers measurements were selected for modeling in this paper.

Table 1. The explained variance value of the SSB estimations for different datasets

	Cycle 207 (n=8 051)	Cycles 207 and 218 (n=14 203)	Cycles 207, 218, 225 and 234 (n=26 127)
D/cm^2	23.29	23.46	23.67

The explained variance is defined as the difference between the variance of SSH discrepancy without SSB correction and that with the SSB correction which can be understood as the part of the variance of the SSH discrepancy that can be explained by the SSB. The higher the explained variance value is, the more effective the model is (Miao et al., 2015).

3.2 *Determination of SSB estimated value $\varphi(x_1)$ at the ascending arc of crossover points*

In order to obtain the estimation $\varphi(x)$ of any measurement x by Eq. (8), the value of $\varphi(x_1)$ should be estimated first (Gaspar and Florens, 1998; Gaspar et al., 2002).

Setting $x = x_{1j}$, Eq. (8) can be rewritten as

$$\varphi(x_{1j}) = \sum_{i=1}^{n}[y_i\alpha_n(x_{1j} - x_{2i})] + \sum_{i=1}^{n}[\varphi(x_{1i})\alpha_n(x_{1j} - x_{2i})], \quad \forall j = 1, \cdots, n. \tag{15}$$

Equation (15) can be changed to a matrix form

$$(\boldsymbol{I} - \boldsymbol{A})\boldsymbol{\varphi}(\boldsymbol{x}_1) = \boldsymbol{A}\boldsymbol{y}, \tag{16}$$

where $\boldsymbol{I}$ is the $n\times n$ identity matrix; and $\boldsymbol{A}$ is the $n\times n$ matrix with elements $\alpha_{ij}(x_{1j} - x_{2i})$, $\boldsymbol{\varphi}(x_1)^{\mathrm{T}} = [\varphi(x_{11}), \ldots, \varphi(\boldsymbol{x}_{1n})]$, and $\boldsymbol{y}^{\mathrm{T}} = [y_1, \ldots, y_n]$.

Equation (16) cannot be solved for $\boldsymbol{\varphi}(x_1)$ because $\boldsymbol{I} - \boldsymbol{A}$ is a singular matrix. The definition of the weights [Eq. (7)] implies that the sum of elements is 0 in each line of this matrix. We have to impose (rather than calculate) one value of $\boldsymbol{\varphi}(x_1)$, that is, φ_{11} is the first element in the data set

$$\varphi(x_{11}) = \varphi_0. \tag{17}$$

So Eq. (16) can be rewritten as

$$\boldsymbol{B}_1\boldsymbol{\varphi} = \boldsymbol{A}\boldsymbol{y} - \boldsymbol{B}_0\varphi_0, \tag{18}$$

where $\boldsymbol{\varphi}$ is the vector made by the n–1 components of $\boldsymbol{\varphi}(\boldsymbol{x}_1)$; $\boldsymbol{\varphi}^{\mathrm{T}} = [\varphi(x_{12}), \ldots, \varphi(x_{1n})]$, and $(\boldsymbol{B}_0, \boldsymbol{B}_1)$ is a partitioned matrix of $\boldsymbol{I} - \boldsymbol{A}$. We now have a system of n equations with n–1 unknowns. A linear least squares matrix is readily obtained

$$\hat{\boldsymbol{\varphi}} = (\boldsymbol{B}_1^{\mathrm{T}}\boldsymbol{B}_1)^{-1}\boldsymbol{B}_1^{\mathrm{T}}(\boldsymbol{A}\boldsymbol{y} - \boldsymbol{B}_0\varphi_0). \tag{19}$$

This provides the values of $\boldsymbol{\varphi}(x_{1i})$ with i=2, ..., n and we can then get the SSB estimates $\boldsymbol{\varphi}(x_1)$ at the ascending arc with $\boldsymbol{\varphi}(x_{11})$ (generally it takes any reasonable value, such as –0.05 m for the first element value).

4 Results and discussion

The ascending arc estimates of the SSB at the crossover of Jason-2 Cycle 207 was obtained firstly, then the corresponding descending arc estimates of the SSB can be obtained by Eq. (8). The efficiency of nonparametric model can be verified by the explained variance, the correlation between the SSB and the SWH or wind speed and the residual of the model.

The SSB is a function of the SWH and the wind speed, such that the model is effective only when the correlation between the SSB and the SWH or wind speed is high. This paper analyzed the correlation degree (r^2) between the SSB and the SWH or wind speed to validate the proposed model.

From Eq. (2), the residual (ε) is the difference between the SSH discrepancy and the SSB discrepancy at the crossover points. The SWH discrepancy was sorted with 0.5 m interval and the wind speed discrepancy with 0.5 m/s interval. The mean value ($\bar{\varepsilon}$) of the residual was calculated and the correlation with Δh_{s} or ΔU was analyzed. The model will be more effective if the correlation between $\bar{\varepsilon}$ and Δh_{s} or ΔU is weak and the absolute deviation and standard deviation (std) of $\bar{\varepsilon}$ are smaller in each section.

4.1 *Optimization selection of different nonparametric SSB estimated models*

Two nonparametric methods, NW or LLR, both can be used to estimate the SSB. The global bandwidth, h_U=0.7 m/s and $h_{h_{\mathrm{s}}}$= 0.3 m, can be calculated by Eq. (13). We can selected $h_U = 2.0$ m/s and $h_{h_{\mathrm{s}},0} = 0.9$ m as the initial bandwidth which are the locally variable bandwidths and can be calculated by Eq. (14). By using the Gaussian kernel function or the spherical Epanechnikov kernel function, and selecting different forms of bandwidth, eight nonparametric models of estimating SSB can be established. The results are shown in Table 2. As shown in Table 2, the SSB estimates are different corresponding to different estimation methods. According to the explained variance (D), the LLR estimation is better than the NW estimation and the locally variable bandwidth is better than the global bandwidth. The nonparametric model which is based on the LLR estimation, the spherical Epan-

Table 2. Evaluation of different nonparametric models

	$K(\cdot)$	h_x	b		D/cm^2	r^2		$\bar{\varepsilon}$-Δh_s		$\bar{\varepsilon}$-ΔU	
			mean/cm	std/cm		b-h_s	b-U	mean/cm	std/cm	mean/cm	std/cm
NW	G	G	–7.97	3.14	20.67	0.86	0.63	–0.80	4.00	0.39	1.60
		L	–8.25	3.27	21.23	0.86	0.80	–0.35	4.00	0.35	1.40
	E	G	–10.63	4.16	23.29	0.90	0.70	0.52	2.71	1.56	1.00
		L	–9.61	4.28	23.58	0.91	0.70	–0.91	2.64	0.07	0.96
LLR	G	G	–9.35	4.55	24.30	0.93	0.63	–1.52	2.48	–0.47	0.95
		L	–9.36	4.59	24.60	0.91	0.64	–1.46	2.23	–0.46	0.94
	E	G	–10.76	4.67	24.12	0.91	0.61	0.53	2.43	1.21	0.95
		L	–11.22	4.85	24.72	0.93	0.80	–0.29	2.43	0.36	0.94

Note: In $K(\cdot)$, G is abbreviated from Gaussian and E is abbreviated from Epanechnikov; and in h_x, G represents h_Global and L represents h_Local.

echnikov kernel function and the locally variable bandwidth (hereafter referred to as LLR-E-L) lead to significant improved results. In this model, the r^2 has higher values (0.93, 0.80) and the mean and standard deviations of ε with respect to Δh_s and ΔU are relatively smaller.

Further analysis of the different nonparametric methods from theory was carried out by Labroue et al. (2004) and Scharoo and Lillibridge (2004), the same conclusions can be obtained with the above results.

(1) The NW estimation is a local constant estimation. The rate of convergence is slow at a boundary point than that at an interior point which is called boundary effect. While the LLR estimation is a local function estimation which can effectively eliminate the boundary errors.

(2) By using the Epanechnikov kernel function to replace the Gaussian kernel function, we can transform the huge linear matrix into a sparse matrix which can greatly improve the computation efficiency.

(3) Bandwidth is the main parameter that affects the accuracy of the nonparametric estimation. Too large bandwidth leads to a smooth regression curve, and the results close to the parameters. Too small bandwidth leads to a rough regression curve, which means that random errors are hard to be excluded. The selection of bandwidth must be appropriate. By using the locally variable bandwidth to replace the global bandwidth, we can improve the smoothing based on the data density which has obvious advantages in the data-sparse regions.

4.2 *Comparisons between LLR-E-L and PM at different latitudes*

4.2.1 *Analysis of sea state at different latitudes*

We have divided the data of Cycle 207 into three latitude ranges, the north latitudes [+20°, 66°), the mid-latitudes [–20°, +20°) and the south latitudes (–66°, –20°). The average and standard deviations of the SWH and the wind speed were calculated respectively in each latitude ranges as shown in Table 3.

Table 3. Statistics of SWH and wind speed at different latitudes

	n	h_s		U	
		mean/m	std/m	mean/m·s^{-1}	std/m·s^{-1}
North latitudes [+20°, 66°)	1 545	3.67	1.56	10.27	4.29
Mid-latitudes [–20°, +20°)	822	1.93	0.61	6.24	2.32
South latitudes (–66°, –20°)	5 602	2.93	1.12	8.67	3.44

As shown in Table 3, the sea states are different at different latitudes. Both SWH and wind speed are large at north latitudes while the SWH and the wind speed are small and steady at mid-latitudes. These will cause large differences of the SSB at different latitudes.

4.2.2 *Analysis for SSB estimated models at different latitudes*

We selected the following six-parameter form as the parametric model (PM) (Gasper et al., 1994):

$$b = h_s[a_1 + a_2 h_s + a_3 U + a_4 {h_s}^2 + a_5 U^2 + a_6 h_s U]. \quad (20)$$

Based on the data set $\left[\Delta h', \Delta h_s, \Delta({h_s}^2), \Delta(h_s U), \Delta({h_s}^3), \Delta(h_s U^2), \Delta({h_s}^2 U)\right]$, the coefficients of the PM can be calculated by a least square fit as shown in Table 4.

Both the LLR-E-L and the PM were established based on full latitude data set which then were used to estimate the SSB in the above three latitude ranges. The results are shown in Table 5. From Table 5, the explained variances are significant different at different latitudes for either LLR-E-L or PM model because of different sea-state effects. At the mid-latitudes, the SWH and the wind speed are smaller and the induced SSB is smaller. The SWH and the wind speed at the south latitudes are larger but not complicated because of the vast ocean. But at the north latitudes, the sea state is relative complicated due to the land distribution. Accordingly, the nonparametric model LLR-E-L performs well at north latitudes. Its explained variance value (33.25 cm^2) is the largest in all. The correlations between the SSB and the SWH or wind speed in the LLR-E-L are higher than those in the PM, especially the correlation between the SSB and the wind speed and the residual distribution is also better than that of the PM. Compared with the PM, the LLR-E-L has no significant advantages at the mid-latitudes and south latitudes. So the PM should be used to estimate the SSB in these two regions considering the computation efficiency.

Table 4. Coefficients of PM

a_1	a_2	a_3	a_4	a_5	a_6
–0.054 700	0.006 600	–0.002 500	–0.000 503	0.000 061	0.000 153

Scatter plots and residual plots between the SSB and the SWH or wind speed for two models at north latitudes are shown

Table 5. Results of SSB LLR-E-L and PM at different latitudes

		b		D/cm^2	r^2		$\bar{\varepsilon}$-Δh_s		$\bar{\varepsilon}$-ΔU	
		mean/cm	std/cm		b-h_s	b-U	mean/cm	std/cm	mean/cm	std/cm
North latitudes [+20°, 66°)	LLR-E-L	–18.20	5.78	33.25	0.89	0.77	0.01	1.58	0.98	1.01
	PM	–17.67	5.63	31.20	0.95	0.53	–0.60	3.93	1.30	1.73
Mid-latitudes [–20°, +20°)	LLR-E-L	–6.93	2.37	4.70	0.82	0.65	2.67	3.47	3.99	5.43
	PM	–10.51	3.08	4.94	0.97	0.52	1.09	3.32	1.58	2.24
South latitudes (–66°, –20°)	LLR-E-L	–10.58	3.80	24.45	0.88	0.68	0.99	4.11	1.58	1.68
	PM	–15.00	4.63	25.77	0.96	0.55	0.21	1.88	0.56	0.88

in Figs 1–4. The results show that the nonparametric model LLR-E-L performs better at north latitudes. Especially, the SSB and the wind speed variabilities have been improved significantly.

5 Application of LLR-E-L in HY-2A altimeter

Both the nonparametric model LLR-E-L (NP) and the parametric model (PM) are used to estimate the SSB of Cycles 70 and 71 (June, 2014) for HY-2A altimeter in the above three latitude ranges. The ascending arc estimates of the SSB at the crossover (n=6 000) were obtained firstly, then the corresponding descending arc estimates of the SSB can be obtained by Eq. (8). The coefficients of the PM can be fitted by crossovers data set of Cycles 70 and 71. The results of two models are shown in Table 6. From Table 6, the explained variance are significantly different at different latitudes because of different sea-state effects. At the mid-

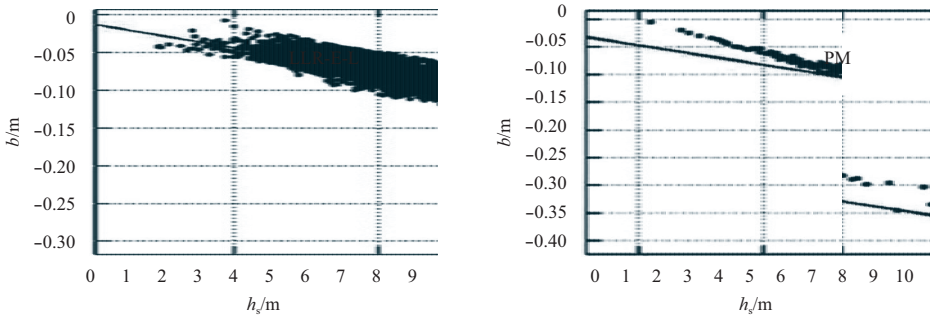

Fig. 1. Scatter plots of the relationship between the SSB and the SWH at north latitudes.

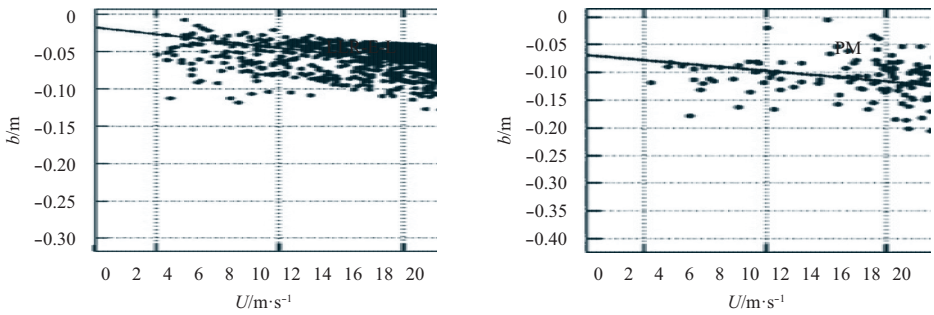

Fig. 2. Scatter plots of the relationship between the SSB and the wind speed at north latitudes.

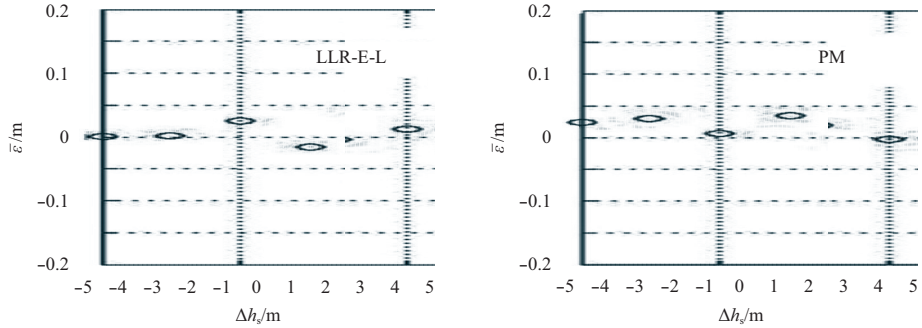

Fig. 3. Mean residuals $\bar{\varepsilon}$ distributions according to Δh_s at north latitudes.

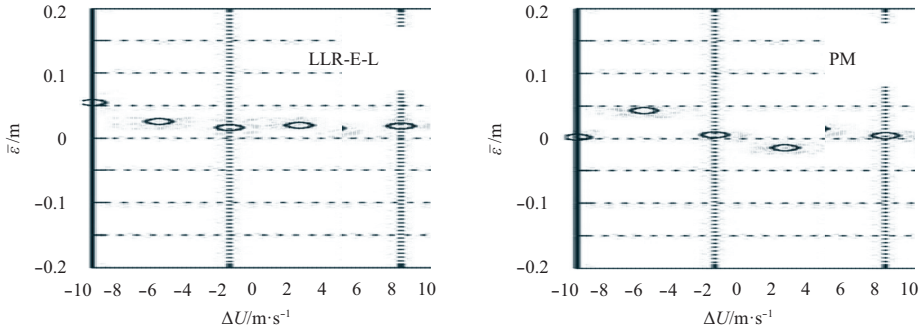

Fig. 4. Mean residuals $\bar{\varepsilon}$ distributions according to ΔU at North latitudes.

Table 6. Results of SSB for NP and PM in different latitudes at HY-2A

		b		D/cm^2	r^2		$\bar{\varepsilon}$-Δh_s		$\bar{\varepsilon}$-ΔU	
		mean/cm	std/cm		b-Δh_s	b-U	mean/cm	std/cm	mean/cm	std/cm
north latitudes [+20°, 66°)	NP	–17.25	4.78	32.12	0.88	0.87	0.02	1.35	0.88	1.11
	PM	–16.65	4.87	29.25	0.92	0.56	0.65	3.86	1.40	1.83
mid-latitudes [–20°, +20°)	NP	–7.95	2.39	4.75	0.85	0.75	2.57	3.58	3.89	5.87
	PM	–11.53	3.56	4.90	0.95	0.54	1.05	3.38	1.46	2.23
south latitudes (–66°, –20°)	NP	–11.58	3.90	25.62	0.89	0.67	0.89	4.78	1.38	1.87
	PM	–14.12	4.34	26.55	0.92	0.56	0.28	1.67	0.78	0.95

latitudes, the SWH and the wind speed are smaller and the induced SSB is smaller. The nonparametric model performs well at the north latitudes. Its explained variance value (32.12 cm^2) is largest in all, the correlations between the SSB and the SWH or wind speed are higher (0.88, 0.87), and the mean and standard deviations of residual distributions (ε-Δh_s, ε-ΔU) are smallest in the three different latitudes. At the mid-latitudes and the south latitudes, the nonparametric model has no significant advantages except the correlation between the SSB and the wind speed. So the nonparametric model is more effective at the north latitudes.

6 Conclusions

(1) In several nonparametric SSB estimation models, the LLR estimation model with the spherical Epanechnikov kernel function and the locally variable bandwidth has significant advantages.

(2) Compared with the parametric model, the nonparametric model significantly improves the correlation between the SSB and the wind speed which makes the wind speed and the SWH have the same effects on the SSB.

(3) The nonparametric model is more effective than the parametric model above 20° N. Considering an estimation accuracy and a computation efficiency, both models have advantages at different latitudes. Thus, different models should be used to estimate the SSB at different latitudes.

References

Feng Hui, Yao Shan, Li Linyuan, et al. 2010. Spline-based nonparametric estimation of the altimeter sea-state bias correction. IEEE Geoscience and Remote Sensing Letters, 7(3): 577–581

Fu L L, Cazenave A. 2001. Satellite Altimetry and Earth Sciences. San Diego: ACADEMIC Press, 1–4

Gaspar P, Florens J P. 1998. Estimation of the sea state bias in radar altimeter measurements of sea level: Results from a new nonparametric method. J Geophys Res, 103(C8): 15803–15814

Gaspar P, Labroue S, Ogor F, et al. 2002. Improving nonparametric estimates of the sea state bias in radar altimeter measurements of sea level, J Atmos Oceanic Technol 19: 1690–1707

Gaspar P, Ogor P, Le Traon P Y, et al. 1994. Estimating the sea state bias of the TOPEX and POSEIDON altimeters from crossover difference. J Geophys Res, 99(C12): 24981–24994

Labroue S, Gaspar P, Dorandeu J, et al. 2004. Nonparametric estimates of the sea state bias for the Jason-1 radar altimeter. Marine Geodesy, 27: 453–481

Li Shuguang, Wang Yunhai, Miao Hongli, et al. 2013. A parametric model of estimating sea state bias based on Jason-1 altimetry. Journal of China University of Petroleum (in Chinese), 37(2): 181–185

Miao Hongli, Wang Xin, Wang Guizhong, et al. 2015. Study on the improved sea state bias parametric estimation model. Periodical of Ocean University of China (in Chinese), 47(12): 119–124

Rami A, Kahlouche S, Haddad M, et al. 2011. Nonparametric estimation of the sea state bias in Jason-1 measurements and their effect on Mediterranean mean sea surface height. International Journal of Academic Research, 3(2): 1024–1028

Scharoo R and Lillibridge J. 2004. Nonparametric sea state bias models and their relevance to sea level change studies. Envisat Symposium Proceedings

Tran N, Labroue S, Philipps S, et al. 2010a. Overview and update of the sea state bias corrections for the Jason-2, Jason-1 and Topex missions. Marine Geodesy, 33: 348–362

Tran N, Vandemark D, Labroue S, et al. 2010b. Sea state bias in altimeter sea level estimates determined by combining wave model and satellite and satellite data. J Geophys Res, 115: 1–7

Vandemark D, Tran N, Beckley B D, et al. 2002. Direct estimation of sea state impacts on radar altimeter sea level measurements. Geophysical Research Letters, 29(24): 48–52

Wang Guizhong, Miao Hongli, Wang Xin, et al. 2014a. Study on parametric model of sea state bias in altimeter based on fusion dataset of collinear and crossover. Remote Sensing Technology and Application, 29(1): 176–180

Wang Jin, Zhang Jie, Fan Chenqing,Wang Jing. 2014b. Validation of the "HY-2" altimeter wet tropospheric path delay correction based on radiosonde data. Acta Oceanologica Sinica, 33(5): 48–53

Ye Xiaomin, Lin Mingsen, Xu Ying. 2015. Validation of Chinese HY-2 satellite radar altimeter significant wave height. Acta Oceanologica Sinica, 34(5): 60–67